Imaging Three-Dimensional Molecular Structure and Dynamics with Multiparticle Covariance and Cumulant Coulomb Explosion Analysis

Chuan Cheng,[†] Yoshiaki Kumagai,[‡] Kiyonobu Nagaya,[¶] Tatsuo Gejo,[§] James Harries,[‖] Michael Burt,[⊥,#] Mark Brouard,[⊥] Avijit Duley,[@] Paul Hockett,[△] Joseph W. McManus,[⊥] Russell S. Minns,[▽] Subhendu Mondal,[††] Shigeki Owada,[‡‡] Weronika Razmus,[▽] Daniel Rolles,[@] Takahiro Sato,[§§] Henry J. Thompson,[▽] Anbu Venkatachalam,[@] Emily M. Warne,[⊥] Tiffany Walmsley,[⊥] Mana Yagi,[§] Philip Bucksbaum,[†] Felix Allum,[†,‖‖‖] and Ruaridh Forbes*[,§§]

†*PULSE Institute, SLAC National Accelerator Laboratory, Menlo Park, California, 94025, USA*

‡*Department of Physics, Nara Women's University, Nara 630-8506, Japan*

¶*Department of Physics, Kyoto University, Kyoto, 606-8502, Japan*

§*Graduate School of Material Science, University of Hyogo, Kouto 3-2-1, Kamigori-cho, Ako-gun, Hyogo 678-1297, Japan*

‖*QST, SPring-8, Kouto 1-1-1, Sayo, Hyogo, 679-5148, Japan*

⊥*Chemistry Research Laboratory, Department of Chemistry, University of Oxford, Oxford, OX1 3TA, UK*

#*Department of Chemistry, Trent University, 1600 West Bank Drive, Peterborough, K9L 0G2, ON, Canada*

@*J.R. Macdonald Laboratory, Department of Physics, Kansas State University, Manhattan, Kansas, 66506, USA*

△*National Research Council of Canada, Ottawa, ON K1A 0R6, Canada*

▽*School of Chemistry and Chemical Engineering, University of Southampton, Highfield, Southampton, SO17 1BJ, UK*

††*Department of Applied Science and Humanities, Haldia Institute of Technology, Haldia - 721657, India*

‡‡*RIKEN SPring-8 Center, Sayo, Hyogo, 679-5148, Japan*

¶¶*Japan Synchrotron Radiation Research Institute, Hyogo, 679-5198, Japan*

§§*LCLS, SLAC National Accelerator Laboratory, Menlo Park, CA 94025, USA*

‖‖‖*Deutsches Elektronen-Synchrotron DESY, Notkestr. 85, 22607 Hamburg, Germany*

⊥⊥*Department of Chemistry, University of California, Davis, CA 95616, USA*

E-mail: ruforbes@ucdavis.edu

Abstract

Coulomb explosion imaging (CEI) provides a direct means of imaging molecular geometry by correlating fragment ion momenta following fragmentation of a molecular polycation. Here, we demonstrate the use of three-body covariance and four-body cumulant analysis to extract three-dimensional structural information from the X-ray–induced Coulomb explosion of tert-butyl iodide (C_4H_9I). Site-selective ionization at the iodine 4d edge with intense femtosecond soft X-ray pulses from an X-ray Free-Electron Laser (XFEL) enables rapid charge buildup and molecular breakup. By correlating ionic fragments in the molecular-frame, we isolate complete dissociation channels and reveal subtle structural changes, such as umbrella-type motion of the branched alkyl chain, during the ionization process. Comparison with point-charge simulations of the Coulomb explosion shows close agreement, validating the approach. These results establish covariance/cumulant mapping as a powerful strategy for imaging complex three-dimensional (3D) molecular structures, and point the way toward time-resolved CEI using both XFEL and tabletop sources for capturing ultrafast structural dynamics.

TOC Graphic

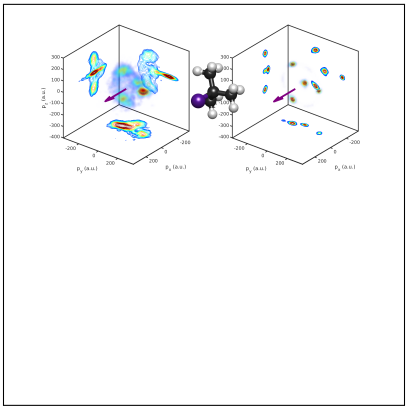

1 Introduction

Structural rearrangements that occur on the femtosecond timescale play a central role in molecular photochemistry, underpinning processes from vision to light harvesting in photosynthesis.[1,2] Tracking these changes in real time to reveal new mechanistic information is a long-standing challenge, requiring tools that can resolve changes in molecular structure on the ultrafast timescale. While time-resolved diffraction techniques, such as electron and X-ray scattering, provide atomically resolved snapshots,[3,4] Coulomb explosion imaging (CEI) has emerged as a powerful and complementary approach.[5–9]

CEI captures structural dynamics by ionizing a molecule into a high charge state, leading to rapid Coulomb-driven fragmentation. The relative momenta of the fragments produced reflect the geometry at the time of the explosion. The ability to initiate Coulomb explosion with femtosecond laser pulses allows observation of transient molecular structures during ultrafast dynamics.[10,11] In recent years, such pump-probe CEI measurements have investigated a range of photochemistry, including photodissociation,[8,12,13] ring-opening,[14] roaming[6] and isomerization.[15] In contrast to diffraction-based methods, CEI is inherently sensitive to light atoms such as hydrogen and can access higher-order nuclear correlations beyond pair distributions.[7,9,16] Moreover, CEI effectively images molecules on a molecule-by-molecule basis. The single-molecule nature of CEI was recently exploited by Richard *et al.* to study correlated ground-state structural fluctuations in an ensemble of molecules of 2-iodopyridine.[17] CEI's high sensitivity has similarly been exploited to image very dilute species, such as weakly bound van der Waals clusters.[18–20]

Although many CEI experiments use intense near-infrared (NIR) pulses to trigger strong-field ionization (SFI),[5,10] recently, X-ray free-electron lasers (XFELs) have opened a new regime for CEI, enabling inner-shell (multiple) photoionization followed by Auger-Meitner decay to rapidly reach high charge states with minimal nuclear distortion.[7,21,22] Compared to SFI-based CEI, this approach mitigates some—but not all—effects associated with field-

driven dynamics (nuclear motion during ionization, sequential charge buildup, coordinate-dependent ionization rates, field-induced dynamics etc.[5,23–28]) and thus provides an alternative pathway to the molecular structure at the moment of ionization by a more faithful mapping of initial geometry to final momenta. Nevertheless, XFEL-driven ionization introduces its own complexities, including rapid multi-step Auger cascades and multi-site ionization,[29] which can blur this mapping.

As molecular size increases, a greater total charge must be deposited to drive a full breakup into atomic ions: while three charges may suffice for a triatomic molecule, considerably higher charge states are required for larger systems such as the 14-atom tert-butyl iodide (the molecule studied in the current work). Achieving these conditions is far more feasible with XFEL-driven inner-shell ionization, where rapid Auger-Meitner cascades can populate high charge states efficiently. In contrast, SFI rates decrease exponentially as ionization potential increases,[30] making it challenging to reach high charge states, given the stepwise increase in ionization potential with each successive electron removed. Particularly given ongoing developments in high repetition-rate XFELs, X-ray induced CEI holds great promise for future studies of ultrafast photochemistry in the gas phase.[8,31–33]

Extending CEI to larger molecules remains a key challenge. To date, most studies have focused on small molecular systems such as triatomics[5,8,19,25,28] or rigid (often planar) polyatomics,[7,17,34] where complete fragmentation pathways can be cleanly identified. In flexible hydrocarbons or substituted systems, however, the combinatorial growth of dissociation channels and reduced detection efficiency for multiple ion coincidences makes it difficult to isolate complete Coulomb explosions.[16] Progress on these challenges is being made on several fronts, including the development of higher-efficiency detectors,[35] the advent of high-repetition-rate light sources,[15,36–38] and advanced data analysis strategies with more differential observables[39–44] capable of extracting genuine structurally informative correlations from noisy, incomplete datasets — the latter being a focus of the present work.

Covariance and cumulant mapping have emerged as powerful tools within CEI.[39–43,45,46]

These statistical analysis methods allow the extraction of correlations among sets of fragments, while mitigating the deleterious effects of 'false coincidences' — contributions from separate molecules ionized in the same laser shot that become increasingly prevalent when recording data in a high count-rate regime. In this work, we apply higher-order covariance/cumulant analysis to XFEL-induced CEI of tert-butyl iodide (C_4H_9I), a prototypical flexible substituted hydrocarbon. We show that three-body correlations provide clean molecular-frame maps of fragment momenta from complete Coulomb explosion events, while four-body cumulants confirm these correlations despite the reduced statistics arising from limited detection efficiencies. Comparison with point-charge CEI simulations reveals subtle umbrella-type carbon motions during the dissociation, demonstrating both the structural sensitivity of this method and its ability to capture dynamics occurring during the explosion itself. The current results establish covariance/cumulant mapping as a powerful strategy for imaging complex and 3D polyatomic molecules, and lay the foundation for high-throughput time-resolved CEI at next-generation high-repetition-rate XFELs.

2 Results

As described in the Methods, site-selective ionization of tert-butyl iodide (C_4H_9I) at the iodine 4d edge with intense femtosecond soft X-ray pulses from SPring-8 Angstrom Compact free-electron LAser (SACLA) XFEL produced rapid multiple ionization and Coulomb explosion. The experimental arrangement is shown schematically in Figure 1. The focused FEL pulses intersect a molecular beam of tert-butyl iodide within a velocity map imaging spectrometer equipped with a delay-line detector. From the recorded hit positions and arrival times, the full 3D fragment momenta were reconstructed. Due to the 60 Hz repetition rate of SACLA, and in order to acquire meaningful statistics within the timeframe of the beamtime, the experiment was carried out at high event rates, with many ions detected per shot (mean: 7.3). This is key in allowing for meaningful multi-particle correlations to be extracted under these low repetition-rate conditions, but, as discussed in detail shortly, necessarily leads to

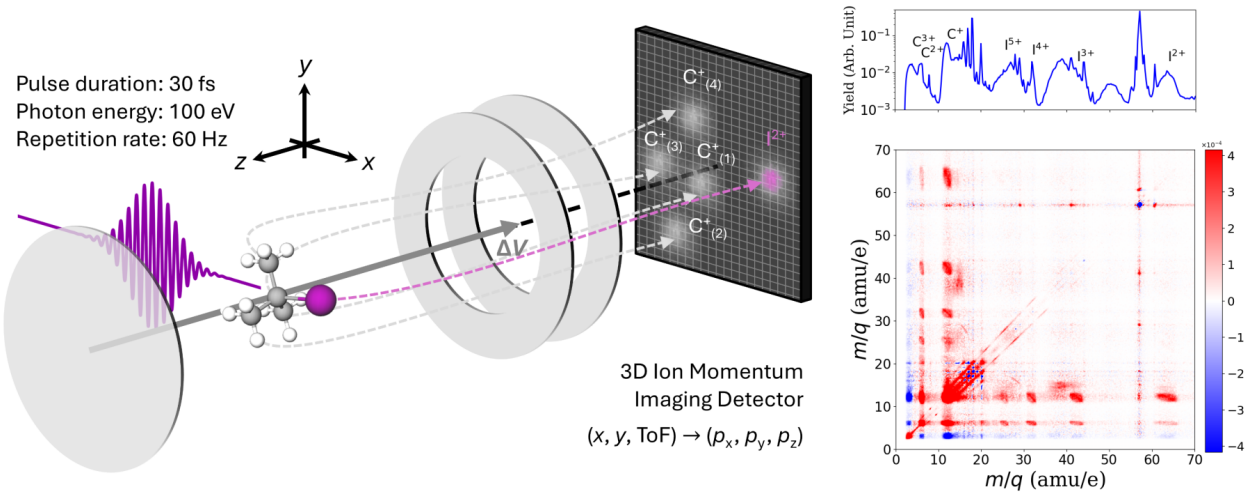

Figure 1: Schematic of the experiment, showing the interaction of a molecular beam of tert-butyl iodide with an intense soft X-ray femtosecond laser pulse. The resultant ions are velocity-mapped to a time- and position-sensitive detector, allowing for the determination of the 3D momentum vector of each detected ion. The right panel shows the ToF-ToF (converted to m/q, i.e. mass-to-charge ratio) covariance map which contains dissociation information about different dissociation channels. The observed ion mass spectrum (plotted on a logarithmic intensity scale) is presented above - with particular atomic ions of interest labelled.

high levels of false coincidences that preclude the use of traditional coincidence analysis.

The rich fragmentation dynamics of this molecule after soft X-ray ionization is highlighted in the time-of-flight (ToF) covariance plot shown in Figure 1, where numerous correlated ion pairs arise from the many accessible dissociation pathways. This combinatorial growth of channels illustrates the challenge of extending CEI beyond small molecules, and motivates the use of higher-order covariance and cumulant mapping to disentangle complete breakups (i.e. into atomic ions) from overlapping or incomplete explosions (i.e. yielding larger molecular and/or neutral fragments). In the following, we focus on high charge state (e.g. (I^{2+} + C^+ + C^+)) and near-complete atomization channels, where the momentum correlations are most directly connected to the underlying equilibrium geometry, enabling imaging of the molecular structure.

By correlating the 3D momenta of three (or four) fragments using covariance and cumulant mapping, the fragmentation dynamics can be analyzed in the molecular-frame.[40,41]

Figure 2 shows the correlated momentum distributions for the three-body breakup channel (I^{2+}, C^+, C^+) in the molecular-frame for experiment (panel (a)) and simulation (panel (b)). In this representation, the I^{2+} momentum is aligned along the $+p_x$ axis (purple arrow), while one of the carbon fragments (C^+, herein denoted as the 'reference') is placed in the p_x-p_y plane ($p_y > 0$, $p_z = 0$). These choices define the I-C axis, and a reference plane, in the molecular-frame. The recoil distribution of both carbon ions are then plotted in this frame, revealing correlations that reflect the original displacement of the atoms in the neutral geometry. In Figure 2, these correlated momentum distributions are represented both as a 3D density plot and are projected as contour plots on each 2D plane. The observed isolated signals, in both experiment and simulation, can immediately be related to each original carbon atom shown in the adjacent molecular structure. If the reference C^+ ion used to define the plane in a given coincidence originates from a terminal carbon (these carbons are symmetric to each other), this choice of molecular-frame effectively fixes the molecular orientation to that shown in Figure 2. This reference carbon, pointing to the right in the page (black arrow), has zero z momentum, and a substantial positive y momentum. The two carbon atoms lying above/below the x/y plane yield C^+ with substantial positive/negative z momentum, whilst the central carbon atom yields C^+ ions with negative momentum in the x dimension and y/z momenta close to zero due to recoil against I^{2+} and equal forces from recoil with three terminal carbons. In the case where the central C atom is used as reference C^+, the relationship between molecular-frame momenta and initial molecular orientation is more complex. This choice leads to molecular-frame signals that are diffuse and broadly distributed. This could be excluded by filtering on a coincidence-by-coincidence basis on the relative recoil angle between the I^+ ion and the reference C^+ used to define the frame.

In the simulations presented in Figure 2(b), a pool of initial geometries was generated from the molecule's equilibrium structure using Gaussian blurring (convolving the position of each atom with a 3D Gaussian with σ=0.1Å) to sample a pool of molecular structures. For comparison, analogous simulations were performed instead using harmonic Wigner sam-

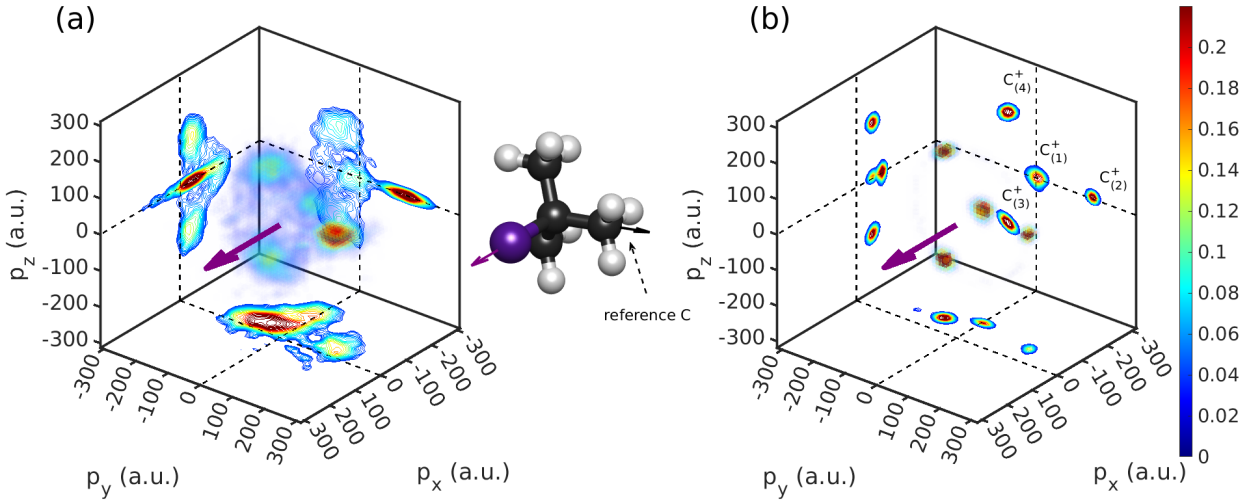

Figure 2: Comparison between the 3D molecular-frame C^+ momentum distribution (in atomic units of momentum, a.u.) from a (I^{2+}, C^+, C^+) correlation extracted from the experimental data (a) and simple simulation (b). The resulting distributions are shown together with contour projections onto each Cartesian plane. The I^{2+} momentum (purple arrow) and reference C^+ momentum (black arrow) are used to define the frame.

pling (assuming a vibrational temperature of 298 K) to generate a pool of initial molecular structures. Generally, the results of these two sets of simulations were qualitatively similar for the representation of relative momenta used in Figure 2 (and throughout the work), and one sampling method does not significantly better reproduce the experimentally observed width (or mean position) of specific features in the correlated momentum patterns. As such, we conclude that the deviations between the experimental data and simple simulations do not primarily originate from how the initial molecular geometry is sampled.

The general agreement between the output of classical point charge simulations of the Coulomb explosion and the experimental correlated momenta help confirm a strong mapping of initial molecular structure to final correlated momenta. In these point-charge simulations, charges are assigned to the atomic positions of the neutral equilibrium geometry, providing a simple but effective model for the Coulomb explosion. For the (I^{2+}, C^+, C^+) channel, the two undetected carbon atoms were treated as singly charged in the simulation, while the hydrogens were not explicitly included to simplify the model; full simulations incorpo-

rating H^+ fragments are provided in the Supplementary Information (SI). While we note that recent work has demonstrated the promise of using H^+ to extract structural information in CEI experiments,[9] in the present experiment, H^+ ions were not efficiently detected due to a strong overlapping stray-light background. As such, our discussion focuses on the detected heavy atoms. Comparison of the simulated molecular-frame momentum distributions with those observed experimentally closely reproduce the measured features across all three projection planes (i.e. in the p_x-p_z plane etc). The agreement between experiment and simulation in Figure 2 indicates that the point-charge model captures much of the essential Coulomb explosion dynamics despite the inherent simplicity of the modeling, which assumes instantaneous ionization to a single charge state and classical motion governed by purely classical Coulombic forces. Possible causes of observed deviations between simulation and experiment beyond these assumptions include effects of molecular geometry sampling in the simulation and the possible contribution of incomplete fragmentations to the experimental data, as we will now discuss in turn.

The generally strong agreement between the experimental data and these simulations suggests that, under the conditions of intense XFEL-based multiple ionization, a three-ion correlation is sufficient to predominantly select out 'complete' Coulomb explosions into atomic ions, which provide the most comprehensive structural information. To further assess the role of partial Coulomb explosions in the experimental (I^{2+}, C^+, C^+) correlation, we compared this to the (I^{2+}, C^+, C^+, C^+) four-fold correlation extracted with cumulant analysis.[41,47] As shown in Figure 3, the four-body case is significantly noisier. As the number of ionic fragments produced in coincidence increases, the likelihood of capturing all correlated fragments decreases due to the limited efficiency of the detector, typically around 25% for each ionic fragment. Improved efficiencies (up to 90%) could be achieved with funnel-type MCPs[35] and higher absolute acceleration fields.[48] In addition, the computational demands of higher-order covariance and cumulant analysis grow rapidly, making four-body correlations inherently more challenging.[47] Consequently, the four-body correlation exhibits substantially

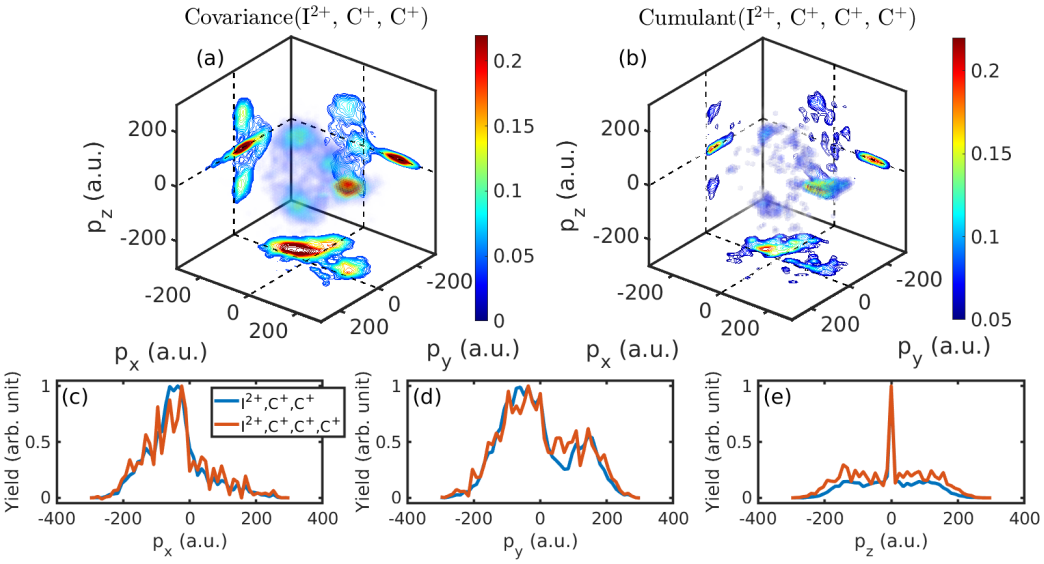

Figure 3: Comparison of the molecular-frame C^+ momentum distributions extracted from (a) a three-body covariance, (I^{2+}, C^+, C^+) and (b) a four-body cumulant (I^{2+},C^+, C^+, C^+). These are represented as described in relation to Figure 2. Additional one-dimensional projections of the three-fold covariance (blue) and four-fold cumulant (red) are presented along (c) p_x, (d) p_y, (e) p_y with each normalized to their own respective maximum value. The similarity between the two correlations indicate that both capture signal from predominantly the same molecular breakup pathway (i.e., total charge state).

higher noise level than the three-body case, and stricter constraints — such as restricting the angle between the I^{2+} momentum and the reference C^+ to 90–135° — to isolate meaningful signals above the noise.

Despite these limitations, the three two-dimensional projections (Figure 3 (c-e)) of both correlations show close agreement, and the C^+ one-dimensional projections along the molecular-frame axes are nearly identical. The only distinction is that the noise level is two to three times higher for the four-body correlation, consistent with the expected 25% detection efficiency. On this basis, we conclude that the three-body covariance can be safely treated as representative of the full (I^{2+}, C^+, C^+, C^+, C^+) breakup. Attempts to compute the five-fold cumulant produced even poorer statistics, reinforcing that the three-body analysis provides the most reliable pathway for structural interpretation in this system. A more detailed exploration of five-fold correlations is beyond the scope of the present work. We also note that recent XFEL-induced CEI work employing lower count rates and coincident analysis at a higher-repetition rate XFEL demonstrated that three-fold atomic ion coincidences were suitable for extracting signal from complete Coulomb explosion channels, with higher-fold coincidences (up to an 8 particle correlation) yielding qualitatively similar, but noisier, results.[7]

Further causes of deviations between the simulated and experimental correlated momenta include the assumptions made in the modeling that the potentials governing the Coulomb explosion are purely Coulombic, and that the final charge state is populated instantly. CEI is known to provide the most reliable structural information when probing high parent ion charge states, where the dynamics are dominated by Coulombic repulsion (i.e., contributions from bonding are lessened[49]) and the mapping from initial geometry to final fragment momenta is more direct.[50] In Figure 4, we compare the molecular-frame momentum distributions from the (I^{2+}, C^+, C^+), (I^{3+}, C^+, C^+), (I^{4+}, C^+, C^+), and (I^{4+}, C^{2+}, C^+; where C^{2+} is the reference C^{m+}) covariances (black) with point-charge simulations of a Gaussian-blurred pool of geometries around the equilibrium structure (red). It can be firstly

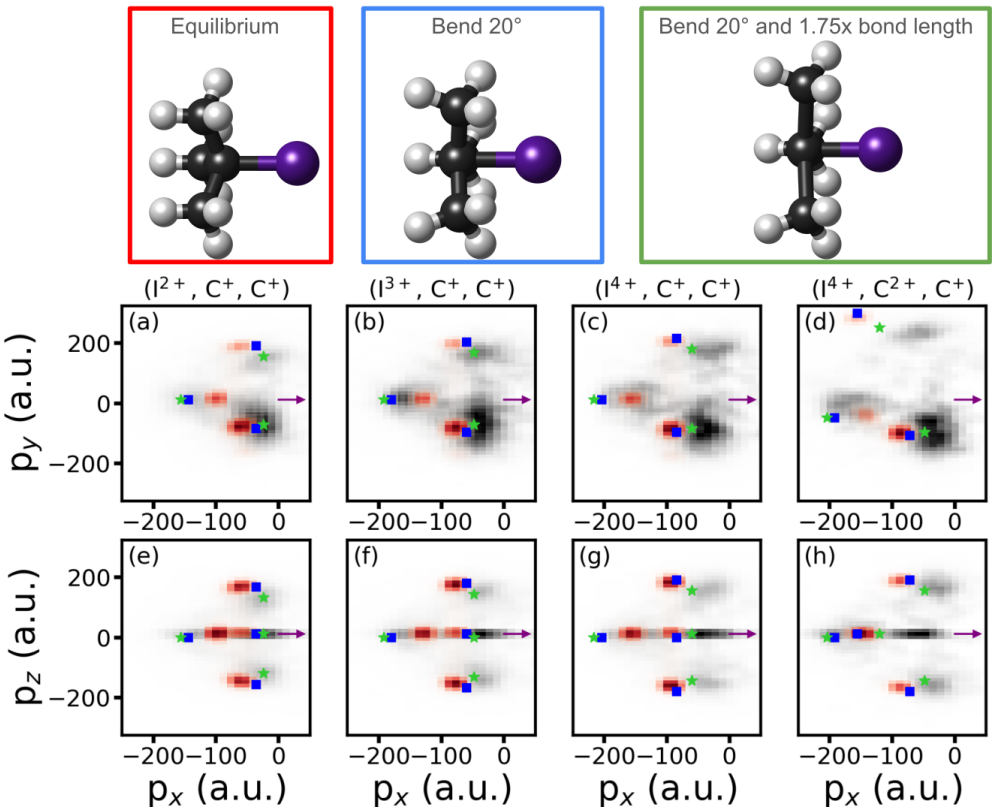

Figure 4: Comparison between experimentally obtained molecular-frame C^{n+} momentum distributions (black shaded region) from 3-body correlations: (a)/(e) (I^{2+}, C^+, C^+), (b)/(f) (I^{3+}, C^+, C^+), (c)/(f) (I^{4+}, C^+, C^+) and (d)/(h) (I^{4+}, C^{2+}, C^+, where C^{2+} is the reference) in the p_x–p_y ((a) to (d)) and p_x–p_z planes ((e) to (h)). Molecular-frame C^{n+} momentum distributions from point-charge Coulomb explosion simulations with a Gaussian blurring around the equilibrium geometry (red region), single bent geometry (blue squares), single bent and stretched geometry (green stars) are also plotted in each projection. The mean geometries used in each simulation are also shown in the plots and described in more detail in the main text.

seen that, as expected, with increasing charges the absolute momenta of the ions increases. Consequently, the distinct islands of signal become increasingly separated for Coulomb explosions from higher total parent charge states. The general shapes of the experimental molecular-frame momentum distributions are reproduced by the classical point-charge simulations (red). However, systematic discrepancies are observed. For instance, the p_x of the signal arising from the terminal carbons are more positive (less negative) in experiment than in simulation (see Figure 4 (a)-(d)). One possible explanation for these differences between the simulation and experiment is nuclear motion occurring during the ionization process, which would break the assumption made in the simulation of an instantaneous Coulomb explosion.[29]

If we are only concerned with the heavy atoms, and preserve the three-fold rotational symmetry, we can consider motion along three coordinates: C—I stretching, I—C—C umbrella motion and C—C stretching. We therefore performed additional Coulomb explosion simulations using geometry-distorted structures to emulate motion along these coordinates during charge build-up. This approach preserves the simplicity of a fixed-geometry instantaneous explosion model. A single-point simulation with the I–C–C angle decreased by 20° from equilibrium is shown as a blue square in each panel. In panel (a), this bent geometry yields significantly better agreement with the experiment, supporting the importance of bending motion in CEI. However, as we progress from (a) to (c), the mismatch in the p_x distribution becomes more pronounced, and by panel (d) the improvement is negligible, indicating that bending alone is insufficient. To achieve closer agreement with the experimental data, we introduced an additional structural change by extending all the C–C bond length to 1.75× its equilibrium value while maintaining the 20° bend. The chosen bond extension is not arbitrary. It was determined empirically to yield the best match to the experimental patterns in panel (a). While this configuration provides a physically plausible and quantitatively improved description, we note that alternative geometries could, in principle, produce similar momentum signatures; thus, the extracted structure should be viewed as represen-

tative rather than unique.[51] Nonetheless, the agreement diminishes at higher charge states, suggesting that the degree of geometry distortion required to capture the finer details of the momentum-frame momentum distributions is charge-state dependent.

Two factors may explain the discrepancies observed. First, at lower charge states, underlying potential energy surfaces are known to exhibit marked deviations from Coulombic behavior, particularly at short bond lengths where bonding interactions still remain.[49,52] Second, the finite duration of the X-ray pulse means that charge is built up sequentially during ionization, so different charge states are reached at different times.[22,53] During this charging window, nuclei can begin to move, particularly the hydrogens, whose dynamics are very fast, and even carbon motion cannot be considered frozen on tens-of-femtoseconds timescales. Recent work using ∼10 fs FEL pulses has already suggested that shorter X-ray pulses substantially improve the structural fidelity of CEI,[7,9] and further reduction of pulse duration will likely be key to recovering more accurate molecular geometries in larger systems. More advanced simulation of X-ray ionization, Auger-Meitner decay and charge motion during the charge up process can also help understand the structures retrieved from CEI analysis and the dynamics of the X-ray induced Coulomb explosion itself.[22,54–56]

The omission of hydrogen atoms in the simulations suggests that they are not essential to reproduce the main features of the heavy ion momenta distributions following Coulomb explosion. When included, their primary effect is to slightly reduce the absolute momenta of the heavier fragments (see SI for further details). This behavior reflects the fact that, once the molecule is highly charged, protons escape much more rapidly than carbons and thus have little influence on the final momenta of the heavier ions. This is compounded by the fact that Coulombic repulsions from H^+ ions impart little impulse on heavier ions due to the light mass of H^+. However, when a large number of hydrogens are present, their collective Coulomb field can measurably modify the momentum partitioning among heavy fragments.[57] A complete understanding of the molecular breakup would require measuring the proton momenta as well. In practice, hydrogen fragments are difficult to detect in the

current FEL setup due to a strong scattered light background early in the ToF window. This effect makes assessing their roles challenging experimentally in the present work.

We have demonstrated that multiparticle covariance and cumulant mapping provide a robust method for extracting 3D structural information from Coulomb explosion imaging of flexible polyatomic molecules. Using tert-butyl iodide as a benchmark system, we showed that three-body covariance maps yield clear molecular-frame recoil patterns, while four-body cumulants validate these correlations, despite reduced statistics. Comparison with point-charge simulations revealed subtle umbrella-type carbon motions prior to dissociation, underscoring the sensitivity of the method to structural rearrangements that occur during ionization. In future work, these dynamics could be minimized by employing shorter X-ray pulses, and a systematic exploration of the influence of pulse properties on Coulomb explosion images will be an important direction.

Overall, our results highlight the power of covariance-based analysis to overcome the limitations of coincidence detection in complex systems, enabling meaningful structural insights even at the relatively low 60 Hz repetition rate of SACLA. This approach will scale naturally with the advent of high-repetition-rate XFELs, where vastly improved statistics will permit systematic studies of fragmentation pathways and the influence of pulse duration and intensity on Coulomb explosion dynamics. Beyond visualizing static structure, covariance and cumulant mapping opens the door to time-resolved studies of ultrafast structural dynamics in larger or weakly bound molecular systems, establishing a pathway toward routine single-molecule structural imaging on femtosecond timescales.

Methods

Experiments were performed at the soft X-ray beamline (BL1) of SACLA, Japan, delivering ∼30 fs XUV pulses at 100 eV photon energy (12.4 nm) with a 60 Hz repetition rate.[58] The horizontally polarized FEL pulses were attenuated using a 1μm Zr filter, resulting in an estimated on-target pulse energy of 2.3 μJ. The XUV beam was focused to a ∼10 μm

spot ($1/e^2$), corresponding to an intensity of 7.6×10^{13} W/cm^2. The focused XUV pulses intersected a pulsed molecular beam of neat tert-butyl iodide (C_4H_9I) inside a velocity map imaging (VMI) ion spectrometer, which has been previously described.[59–61] Ionization occurred site-selectively at the iodine 4d edge, given the very large I 4d photoabsorption cross section at the chosen photon energy (∼20-30 Mb[62,63]). Ionic fragments were extracted and detected using a dual microchannel plate with hexanode delay line detector, enabling full 3D ion momentum reconstruction.

The experimental data analyzed in the present work was recorded during a pump-probe experiment, which also used a ∼121 µJ 800 nm femtosecond laser pulse, generated from the output of the SACLA Ti:Sapphire pump-probe laser. While the pump-probe delay-dependent experiments will be reported in a separate publication, the present work averaged data over all pump-probe delays (covering delays in which either the X-ray or NIR pulse arrived first). As explored in more detail in the SI, the ion momentum correlations analyzed in the present work are expected to originate almost entirely from X-ray ionization of the molecule without influence of the NIR laser. This is supported by comparisons to data recorded irradiating tert-butyl-iodide with the X-ray pulses only. There were 1,973,610 shots collected in total (about 9-10 hours of data acquisition).

To extract structural information from the measured ion momenta, we employed covariance and cumulant mapping techniques.[40–42,47] In high-count-rate FEL experiments, conventional coincidence analysis is impractical due to false coincidences and limited detection efficiency. At the current repetition rate (60 Hz), reducing the total count rate to decrease the contribution from false coincidences would result in a very low total data volume. Instead, covariance analysis provides a statistical measure of correlated fragment emission by evaluating deviations of ion counts from their mean values on a shot-to-shot basis. Using full 3D momentum distributions from the VMI spectrometer, we computed three-body covariances and four-body cumulants from the full 3D momentum distributions obtained with the VMI spectrometer, enabling us to distinguish genuine multi-particle breakups from uncor-

related background. This approach provides access to molecular-frame correlation patterns and allows recovery of 3D structural signatures even in complex polyatomic fragmentations. The details of the computation of these covariances/cumulants has been described in detail previously,[40,41,47] and used the PyCorrCPI Python package.[64] This package enables the calculation of three- and four-fold correlations using recently-developed approaches to improve the efficiency in estimating terms in each covariance/cumulant expression[47] and supports different representations of the extracted correlated 3D ion momentum distributions.

The classical Coulomb explosion simulations were performed using the PyCESim Python package.[65] In short, atomic ions were placed at the corresponding atomic coordinates from an initial molecular structure. Treating the atomic ions as point charges and using Coulomb's law allowed the forces between the ions to be defined, and their trajectories propagated by numerically solving Newton's equations. Simulations were then typically repeated for a pool of initial starting geometries, which were sampled either from a series of 3D Gaussian functions centered at each atomic position or using harmonic Wigner sampling, as described in the main text. The output of these simulations, asymptotic 3D momenta for each ion, were then transformed into the molecular-frame on an explosion-by-explosion basis. Finally, in order to better compare the resultant 3D relative momentum distributions to those recorded experimentally, which are affected by the spectrometer's finite momentum resolution, the resultant covariant/cumulant histogram (which is represented here with 6 a.u. momentum bins) was convolved in 3D. This convolution was performed with a 3x3 cube, with value of 1 in the center voxel, 1/3 at the faces of the cube, 1/9 at the edges and 1/27 at the corners.

Acknowledgements

The experiment was carried out at SACLA with the approval of JASRI and the program review committee (proposal No. 2023A8043 Forbes). We thank the technical and scientific staff of SACLA for their hospitality and support before and during the beamtime. R.F. and F.A. gratefully acknowledge support from the Linac Coherent Light Source, SLAC National

Accelerator Laboratory, which is supported by the US Department of Energy, Office of Science, Office of Basic Energy Sciences, under contract no. DE-AC02-76SF00515. D.R. was supported by contract no. DE-FG02-86ER13491 from the same funding agency. R.S.M. thanks the EPSRC (EP/R010609/1 and EP/X027635/1) and Leverhulme Trust (RPG-2021-257) for financial support. M.B. and J.M. are grateful to EPSRC Programme grant EP/V026690/1. M.Bu., E.M.W. and T.W. are also grateful to EPSRC for support from EP/S028617/1. T.W. is additionally thankful to EPSRC for studentship funding and Jesus College, Oxford for a partial fee scholarship. W.O.R. and H.J.T. thank the UK XFEL hub for physical sciences and the University of Southampton for studentships. P.H.B. and C.C. were supported by the National Science Foundation. S.M. gratefully acknowledges financial support from the JSPS Bridge Fellowship for Research in Japan.

References

(1) Kukura, P.; McCamant, D. W.; Yoon, S.; Wandschneider, D. B.; Mathies, R. A. Structural Observation of the Primary Isomerization in Vision with Femtosecond-Stimulated Raman. *Science* **2005**, *310*, 1006–1009.

(2) Zaharieva, I.; Dau, H.; Haumann, M. Sequential and Coupled Proton and Electron Transfer Events in the $S_2 \rightarrow S_3$ Transition of Photosynthetic Water Oxidation Revealed by Time-Resolved X-ray Absorption Spectroscopy. *Biochemistry* **2016**, *55*, 6996–7004.

(3) Odate, A.; Kirrander, A.; Weber, P. M.; Minitti, M. P. Brighter, Faster, Stronger: Ultrafast Scattering of Free Molecules. *Advances in Physics: X* **2023**, *8*, 2126796.

(4) Centurion, M.; Wolf, T. J.; Yang, J. Ultrafast Imaging of Molecules with Electron Diffraction. *Annual Review of Physical Chemistry* **2022**, *73*, 21–42.

(5) Légaré, F.; Lee, K. F.; Litvinyuk, I. V.; Dooley, P. W.; Wesolowski, S. S.; Bunker, P. R.;

Dombi, P.; Krausz, F.; Bandrauk, A. D.; Villeneuve, D. M. et al. Laser Coulomb-Explosion Imaging of Small Molecules. *Physical Review A* **2005**, *71*, 013415.

(6) Endo, T.; Neville, S. P.; Wanie, V.; Beaulieu, S.; Qu, C.; Deschamps, J.; Lassonde, P.; Schmidt, B. E.; Fujise, H.; Ibrahim, H. et al. Capturing Roaming Molecular Fragments in Real Time. *Science* **2020**, *370*, 1072–1077.

(7) Boll, R.; Schäfer, J. M.; Richard, B.; Fehre, K.; Kastirke, G.; Jurek, Z.; Schöffler, M. S.; Abdullah, M. M.; Anders, N.; Baumann, T. M. et al. X-ray Multiphoton-Induced Coulomb Explosion Images Complex Single Molecules. *Nature Physics* **2022**, *18*, 423–428.

(8) Unwin, J.; Allum, F.; Britton, M.; Gabalski, I.; Bromberger, H.; Brouard, M.; Bucksbaum, P. H.; Driver, T.; Ekanayake, N.; Garg, D. et al. X-ray Induced Coulomb Explosion Imaging of Transient Excited-State Structural Rearrangements in CS_2. *Communications Physics* **2023**, *6*, 309.

(9) Green, A. E.; Chen, K.; Bhattacharyya, S.; Allum, F.; Usenko, S.; Ashfold, M. N.; Baumann, T. M.; Borne, K. D.; Brouard, M.; Burt, M. et al. Visualizing the three-dimensional arrangement of hydrogen atoms in organic molecules by Coulomb explosion imaging. *Journal of the American Chemical Society* **2025**,

(10) Stapelfeldt, H.; Constant, E.; Corkum, P. B. Wave Packet Structure and Dynamics Measured by Coulomb Explosion. *Physical Review Letters* **1995**, *74*, 3780–3783.

(11) Légaré, F.; Lee, K. F.; Bandrauk, A. D.; Villeneuve, D. M.; Corkum, P. B. Laser Coulomb Explosion Imaging for Probing Ultra-Fast Molecular Dynamics. *Journal of Physics B: Atomic, Molecular and Optical Physics* **2006**, *39*, S503–S518.

(12) Crane, S. W.; Lee, J. W.; Ashfold, M. N.; Rolles, D. Molecular photodissociation dynamics revealed by Coulomb explosion imaging. *Physical Chemistry Chemical Physics* **2023**, *25*, 16672–16698.

(13) Ding, X.; Forbes, R.; Kübel, M.; Lee, K. F.; Spanner, M.; Naumov, A. Y.; Villeneuve, D. M.; Stolow, A.; Corkum, P. B.; Staudte, A. Threshold photodissociation dynamics of NO_2 studied by time-resolved cold target recoil ion momentum spectroscopy. *Journal of Chemical Physics* **2019**, *151*, 174301.

(14) Wang, E.; Bhattacharyya, S.; Chen, K.; Borne, K.; Ziaee, F.; Pathak, S.; Lam, H. V. S.; Venkatachalam, A. S.; Chen, X.; Boll, R. et al. Time-resolved Coulomb explosion imaging unveils ultrafast ring opening of furan. *arXiv preprint arXiv:2311.05099* **2023**,

(15) Bhattacharyya, S.; Wang, E.; Borne, K.; Chen, K.; Venkatachalam, A. S.; Lam, H. V. S.; Ziaee, F.; Pathak, S.; Khmelnitskiy, A.; Carnes, K. D. et al. Delayed Dissociation and Transient Isomerization during the Ultrafast Photodissociation of the Tribromomethane Cation. *The Journal of Physical Chemistry Letters* **2024**, *15*, 12188–12196.

(16) Lam, H. V. S.; Venkatachalam, A. S.; Bhattacharyya, S.; Chen, K.; Borne, K.; Wang, E.; Boll, R.; Jahnke, T.; Kumarappan, V.; Rudenko, A. et al. Differentiating three-dimensional molecular structures using laser-induced coulomb explosion imaging. *Physical Review Letters* **2024**, *132*, 123201.

(17) Richard, B.; Boll, R.; Banerjee, S.; Schäfer, J. M.; Jurek, Z.; Kastirke, G.; Fehre, K.; Schöffler, M. S.; Anders, N.; Baumann, T. M. et al. Imaging collective quantum fluctuations of the structure of a complex molecule. *Science* **2025**, *389*, 650–654.

(18) Wu, J.; Kunitski, M.; Schmidt, L. P. H.; Jahnke, T.; Dörner, R. Structures of N2Ar, O2Ar, and O2Xe dimers studied by Coulomb explosion imaging. *The Journal of Chemical Physics* **2012**, *137*.

(19) Kunitski, M.; Zeller, S.; Voigtsberger, J.; Kalinin, A.; Schmidt, L. P. H.; Schöffler, M.; Czasch, A.; Schöllkopf, W.; Grisenti, R. E.; Jahnke, T. et al. Observation of the Efimov state of the helium trimer. *Science* **2015**, *348*, 551–555.

(20) Schouder, C. A.; Chatterley, A. S.; Madsen, L. B.; Jensen, F.; Stapelfeldt, H. Laser-induced Coulomb-explosion imaging of the CS 2 dimer: The effect of non-Coulombic interactions. *Physical Review A* **2020**, *102*, 063125.

(21) Nagaya, K.; Motomura, K.; Kukk, E.; Takahashi, Y.; Yamazaki, K.; Ohmura, S.; Fukuzawa, H.; Wada, S.; Mondal, S.; Tachibana, T. et al. Femtosecond charge and molecular dynamics of I-containing organic molecules induced by intense X-ray free-electron laser pulses. *Faraday discussions* **2016**, *194*, 537–562.

(22) Li, X.; Rudenko, A.; Schöffler, M. S.; Anders, N.; Baumann, T. M.; Eckart, S.; Erk, B.; De Fanis, A.; Fehre, K.; Dörner, R. et al. Coulomb Explosion Imaging of Small Polyatomic Molecules with Ultrafast X-ray Pulses. *Physical Review Research* **2022**, *4*, 013029.

(23) Hasegawa, H.; Hishikawa, A.; Yamanouchi, K. Coincidence imaging of Coulomb explosion of CS2 in intense laser fields. *Chemical physics letters* **2001**, *349*, 57–63.

(24) Seideman, T.; Ivanov, M. Y.; Corkum, P. B. Role of Electron Localization in Intense-Field Molecular Ionization. *Physical Review Letters* **1995**, *75*, 2819–2822.

(25) Bocharova, I.; Karimi, R.; Penka, E. F.; Brichta, J.-P.; Lassonde, P.; Fu, X.; Kieffer, J.-C.; Bandrauk, A. D.; Litvinyuk, I.; Sanderson, J. et al. Charge resonance enhanced ionization of CO 2 probed by laser Coulomb explosion imaging. *Physical review letters* **2011**, *107*, 063201.

(26) Howard, A.; Cheng, C.; Forbes, R.; McCracken, G.; Mills, W.; Makhija, V.; Spanner, M.; Weinacht, T.; Bucksbaum, P. Strong-field ionization of water: Nuclear dynamics revealed by varying the pulse duration. *Physical Review A* **2021**, *103*, 043120.

(27) Cheng, C.; Streeter, Z. L.; Howard, A. J.; Spanner, M.; Lucchese, R. R.; McCurdy, C. W.; Weinacht, T.; Bucksbaum, P. H.; Forbes, R. Strong-field ionization

of water. II. Electronic and nuclear dynamics en route to double ionization. *Physical Review A* **2021**, *104*, 023108.

(28) Ashrafi-Belgabad, A.; Karimi, R.; Monfared, M.; Tian, K.; Parvin, P.; Wales, B.; Bisson, É.; Beaulieu, S.; Giguère, M.; Kieffer, J.-C. et al. Reconstructing Real-Space Geometries of Polyatomic Molecules Undergoing Strong Field Laser-Induced Coulomb Explosion. *Communications Physics* **2024**, *7*, 405.

(29) Takanashi, T.; Nakamura, K.; Kukk, E.; Motomura, K.; Fukuzawa, H.; Nagaya, K.; Wada, S.-i.; Kumagai, Y.; Iablonskyi, D.; Ito, Y. et al. Ultrafast Coulomb explosion of a diiodomethane molecule induced by an X-ray free-electron laser pulse. *Physical Chemistry Chemical Physics* **2017**, *19*, 19707–19721.

(30) Ammosov, M. V.; Delone, N. B.; Krainov, V. P. Tunnel ionization of complex atoms and atomic ions in electromagnetic field. High intensity laser processes. 1986; pp 138–141.

(31) Walter, P.; Holmes, M.; Obaid, R.; Amores, L.; Cheng, X.; Cryan, J. P.; Glownia, J. M.; Li, X.; Lin, M.-F.; Ng, M. L. et al. The DREAM Endstation at the Linac Coherent Light Source. *Applied Sciences* **2022**, *12*, 10534.

(32) Jahnke, T.; Mai, S.; Bhattacharyya, S.; Chen, K.; Boll, R.; Castellani, M. E.; Dold, S.; Duley, A.; Frühling, U.; Green, A. E. et al. X-ray Coulomb explosion imaging reveals role of molecular structure in internal conversion. *arXiv preprint arXiv:2405.15367* **2024**,

(33) Li, X.; Boll, R.; Vindel-Zandbergen, P.; González-Vázquez, J.; Rivas, D. E.; Bhattacharyya, S.; Borne, K.; Chen, K.; De Fanis, A.; Erk, B. et al. Imaging a light-induced molecular elimination reaction with an X-ray free-electron laser. *Nature Communications* **2025**, *16*, 7006.

(34) Yuan, H.; Gao, Y.; Yang, B.; Gu, S.; Lin, H.; Guo, D.; Liu, J.; Zhang, S.; Ma, X.; Xu, S.

Coulomb explosion imaging of complex molecules using highly charged ions. *Physical Review Letters* **2024**, *133*, 193002.

(35) Fehre, K.; Trojanowskaja, D.; Gatzke, J.; Kunitski, M.; Trinter, F.; Zeller, S.; Schmidt, L. P. H.; Stohner, J.; Berger, R.; Czasch, A. et al. Absolute ion detection efficiencies of microchannel plates and funnel microchannel plates for multi-coincidence detection. *Review of Scientific Instruments* **2018**, *89*.

(36) Pullen, M. G.; Wolter, B.; Le, A.-T.; Baudisch, M.; Hemmer, M.; Senftleben, A.; Schröter, C. D.; Ullrich, J.; Moshammer, R.; Lin, C.-D. et al. Imaging an aligned polyatomic molecule with laser-induced electron diffraction. *Nature Communications* **2015**, *6*, 7262.

(37) Rothhardt, J.; Hädrich, S.; Shamir, Y.; Tschnernajew, M.; Klas, R.; Hoffmann, A.; Tadesse, G. K.; Klenke, A.; Gottschall, T.; Eidam, T. et al. High-repetition-rate and high-photon-flux 70 eV high-harmonic source for coincidence ion imaging of gas-phase molecules. *Optics express* **2016**, *24*, 18133–18147.

(38) Ertel, D.; Schmoll, M.; Kellerer, S.; Jäger, A.; Weissenbilder, R.; Moioli, M.; Ahmadi, H.; Busto, D.; Makos, I.; Frassetto, F. et al. Ultrastable, high-repetition-rate attosecond beamline for time-resolved XUV–IR coincidence spectroscopy. *Review of Scientific Instruments* **2023**, *94*.

(39) Slater, C. S.; Blake, S.; Brouard, M.; Lauer, A.; Vallance, C.; Bohun, C. S.; Christensen, L.; Nielsen, J. H.; Johansson, M. P.; Stapelfeldt, H. Coulomb-explosion imaging using a pixel-imaging mass-spectrometry camera. *Physical Review A* **2015**, *91*, 053424.

(40) Allum, F.; Cheng, C.; Howard, A. J.; Bucksbaum, P. H.; Brouard, M.; Weinacht, T.; Forbes, R. Multi-Particle Three-Dimensional Covariance Imaging: "Coincidence" Insights into the Many-Body Fragmentation of Strong-Field Ionized D2O. *Journal of Physical Chemistry Letters* **2021**, *12*, 8302–8308.

(41) Cheng, C.; Frasinski, L. J.; Moǧol, G. m. c.; Allum, F.; Howard, A. J.; Rolles, D.; Bucksbaum, P. H.; Brouard, M.; Forbes, R.; Weinacht, T. Multiparticle Cumulant Mapping for Coulomb Explosion Imaging. *Phys. Rev. Lett.* **2023**, *130*, 093001.

(42) Frasinski, L. J. Cumulant mapping as the basis of multi-dimensional spectrometry. *Physical Chemistry Chemical Physics* **2022**, *24*, 20776–20787.

(43) Brandt, A.; Andersson, Å.; Zhaunerchyk, V. Parametric Cumulant Mapping: A Multidimensional Correlation Method for Experiments with High and Fluctuating Event Rates. *Journal of Physics B: Atomic, Molecular and Optical Physics* **2025**,

(44) Venkatachalam, A. S.; Greenman, L.; Stallbaumer, J.; Rudenko, A.; Rolles, D.; Lam, H. V. S. Exploiting correlations in multi-coincidence Coulomb explosion patterns for differentiating molecular structures using machine learning. *arXiv preprint arXiv:2509.03776* **2025**,

(45) Slater, C. S.; Blake, S.; Brouard, M.; Lauer, A.; Vallance, C.; John, J. J.; Turchetta, R.; Nomerotski, A.; Christensen, L.; Nielsen, J. H. et al. Covariance imaging experiments using a pixel-imaging mass-spectrometry camera. *Physical Review A* **2014**, *89*, 011401.

(46) Pickering, J. D.; Amini, K.; Brouard, M.; Burt, M.; Bush, I. J.; Christensen, L.; Lauer, A.; Nielsen, J. H.; Slater, C. S.; Stapelfeldt, H. Communication: Three-fold covariance imaging of laser-induced Coulomb explosions. *The Journal of Chemical Physics* **2016**, *144*.

(47) Cheng, C.; Frasinski, L. J.; Moǧol, G. m. c.; Allum, F.; Howard, A. J.; Bucksbaum, P. H.; Forbes, R.; Weinacht, T. Multiparticle cumulant mapping for Coulomb explosion imaging: Calculations and algorithm. *Phys. Rev. A* **2024**, *109*, 042802.

(48) Takahashi, N.; Adachi, Y.; Saito, M.; Haruyama, Y. Absolute detection efficiencies for keV energy atoms incident on a microchannel plate detector. *Nuclear Instruments and*

Methods in Physics Research Section B: Beam Interactions with Materials and Atoms **2013**, *315*, 51–54.

(49) Corrales, M. E.; Gitzinger, G.; González-Vázquez, J.; Loriot, V.; de Nalda, R.; Banares, L. Velocity map imaging and theoretical study of the Coulomb explosion of CH3I under intense femtosecond IR pulses. *The Journal of Physical Chemistry A* **2012**, *116*, 2669–2677.

(50) Zhou, W.; Ge, L.; Ashfold, M. N. R.; Cooper, G. A.; Vallance, C. Coulomb explosion imaging for gas-phase molecular structure determination: An ab initio trajectory simulation study. *Journal of Chemical Physics* **2020**, *153*, 184201.

(51) Sayler, A.; Eckner, E.; McKenna, J.; Esry, B.; Carnes, K.; Ben-Itzhak, I.; Paulus, G. Nonunique and nonuniform mapping in few-body Coulomb-explosion imaging. *Physical Review A* **2018**, *97*, 033412.

(52) Singh, V.; Cheng, C.; Weinacht, T.; Matsika, S. Quantum contributions to Coulomb-explosion imaging revealed by trajectory-surface-hopping molecular dynamics. *Physical Review A* **2024**, *109*, 052813.

(53) Motomura, K.; Kukk, E.; Fukuzawa, H.; Wada, S.-i.; Nagaya, K.; Ohmura, S.; Mondal, S.; Tachibana, T.; Ito, Y.; Koga, R. et al. Charge and Nuclear Dynamics Induced by Deep Inner-Shell Multiphoton Ionization of CH_3I Molecules by Intense X-ray Free-Electron Laser Pulses. *Journal of Physical Chemistry Letters* **2015**, *6*, 2944–2949.

(54) Jurek, Z.; Son, S.-K.; Ziaja, B.; Santra, R. XMDYN and XATOM: versatile simulation tools for quantitative modeling of X-ray free-electron laser induced dynamics of matter. *Applied Crystallography* **2016**, *49*, 1048–1056.

(55) Berrah, N.; Sanchez-Gonzalez, A.; Jurek, Z.; Obaid, R.; Xiong, H.; Squibb, R.; Osipov, T.; Lutman, A.; Fang, L.; Barillot, T. et al. Femtosecond-resolved observation

of the fragmentation of buckminsterfullerene following X-ray multiphoton ionization. *Nature Physics* **2019**, *15*, 1279–1283.

(56) Kumagai, Y.; Jurek, Z.; Xu, W.; Fukuzawa, H.; Motomura, K.; Iablonskyi, D.; Nagaya, K.; Wada, S.-i.; Mondal, S.; Tachibana, T. et al. Radiation-induced chemical dynamics in Ar clusters exposed to strong X-ray pulses. *Physical review letters* **2018**, *120*, 223201.

(57) Walmsley, T.; Allum, F.; Harries, J. R.; Kumagai, Y.; Lim, S.; McManus, J.; Nagaya, K.; Britton, M.; Brouard, M.; Bucksbaum, P. et al. Distinguishing the XUV-induced Coulomb explosion dynamics of iodobenzene using covariance analysis. *Journal of Physics B: Atomic, Molecular and Optical Physics* **2024**, *57*, 235101.

(58) Owada, S.; Togawa, K.; Inagaki, T.; Hara, T.; Tanaka, T.; Joti, Y.; Koyama, T.; Nakajima, K.; Ohashi, H.; Senba, Y. et al. A soft X-ray free-electron laser beamline at SACLA: the light source, photon beamline and experimental station. *Synchrotron Radiation* **2018**, *25*, 282–288.

(59) McManus, J. W.; Walmsley, T.; Nagaya, K.; Harries, J. R.; Kumagai, Y.; Iwayama, H.; Ashfold, M. N. R.; Britton, M.; Bucksbaum, P. H.; Downes-Ward, B. et al. Disentangling sequential and concerted fragmentations of molecular polycations with covariant native frame analysis. *Physical Chemistry Chemical Physics* **2022**, *24*, 22699–22709.

(60) Allum, F.; Anders, N.; Brouard, M.; Bucksbaum, P.; Burt, M.; Downes-Ward, B.; Grundmann, S.; Harries, J.; Ishimura, Y.; Iwayama, H. et al. Multi-channel photodissociation and XUV-induced charge transfer dynamics in strong-field-ionized methyl iodide studied with time-resolved recoil-frame covariance imaging. *Faraday Discussions* **2021**, *228*, 571–596.

(61) Allum, F.; Kumagai, Y.; Nagaya, K.; Harries, J.; Iwayama, H.; Britton, M.; Bucksbaum, P. H.; Burt, M.; Brouard, M.; Downes-Ward, B. et al. Direct momentum imag-

ing of charge transfer following site-selective ionization. *Physical Review A* **2023**, *108*, 043113.

(62) Saito, N.; Suzuki, I. H. Multiple photoionization in Ne, Ar, Kr and Xe from 44 to 1300 eV. *International Journal of Mass Spectrometry and Ion Processes* **1992**, *115*, 157–172.

(63) Olney, T. N.; Cooper, G.; Brion, C. Quantitative studies of the photoabsorption (4.5–488 eV) and photoionization (9–59.5 eV) of methyl iodide using dipole electron impact techniques. *Chemical physics* **1998**, *232*, 211–237.

(64) Allum, F. PyCorrCPI - corelation analysis for charged-particle imaging experiments. `https://github.com/f-allum/PyCorrCPI`, 2024.

(65) Allum, F. PyCESIM - Python package for the classical simulation of Coulomb explosion. `https://github.com/f-allum/PyCESim`, 2024.